17

Preparation of Deproteinized Human Bone and Its Mixtures with Bio-Glass and Tricalcium Phosphate – Innovative Bioactive Materials for Skeletal Tissue Regeneration

Magdalena Cieslik[1], Jacek Nocoń[2], Jan Rauch[3], Tadeusz Cieslik[4], Anna Ślósarczyk[5], Maria Borczuch-Łączka[6] and Aleksander Owczarek[7]

[1]*Faculty and Institute of Stomatological Materials Science, Medical University of Silesia, Katowice, Bytom,*
[2]*Private Dentistry Practice, Oberhausen,*
[3]*NZOZ – Specialist Dentistry Clinic, Wadowice,*
[4]*Faculty and Clinic of Oral and Maxillofacial Surgery, Medical University of Silesia, Katowice,*
[5]*Faculty of Glass Technology and Amorphous Coatings, AGH - Krakow University of Science and Technology, Kraków,*
[6]*Faculty of Ceramic Technology, AGH - Krakow University of Science and Technology, Kraków,*
[7]*Division of Statistics, Medical University of Silesia, Katowice, Sosnowiec,*
[1,3,4,5,6,7]*Poland*
[2]*Germany*

1. Introduction

Repair of the skeletal system is one of the principal research problems in medical science is closely associated with the field of material engineering. The reasons for using bone implants and grafts include injuries, infections, neoplasms and other hard tissue lesions. Bone replacement materials are predominantly used in medical disciplines such as dentistry, dental surgery, maxillofacial surgery and plastic surgery, as well as in orthopedics and traumatology (Barradas et al., 2011; Kao & Scott, 2007; Precheur, 2007).

From a biological, immunological, and legal point of view, autogenous bone grafting still remains a very popular method in reconstruction following skeletal loss (Block, 2002; Giannoudis et al., 2005). Factors considered in the selection of the source of the bone graft include, among others, the ease of surgical access and the volume of bone mass required (Precheur, 2007). The type of autogenous bone used as a graft (cortical bone vs. cancellous bone) should also be considered. For instance, the higher content of morphogenetic proteins (BMPs) in cortical bone means that grafts of this type induce the process of bone growth more effectively than cancellous bone grafts. Nonetheless, skeletal reconstruction with autogenous bone grafts always requires additional surgical manipulations that constitute an

increased burden to the patient and prolong the duration of the procedure. Another very frequent limitation of using autogenous bone is its poor quality, when there is a skeletal system disorder (e.g. osteoporosis) (Bohner, 2010; Giannoudis et al., 2005). Allogenic implants derived from the structures of human bones can be one alternative to autogenous grafts (Ferreira, 2007). Mineralized (FDBA) and demineralized (DFDBA) forms of such implants, additionally subjected to lyophilization, are most frequently used in reconstructive surgery. An advantage of demineralized bone arises from the fact that the organic bone matrix (collagen fibers) has to be exposed in order to remove its mineral components, and therefore so-called matrix proteins (e.g. morphogenetic proteins) can easily diffuse into the implantation site and work osteoinductively (Barradas et al., 2011). Xenogenic implants also play an important role in reconstructive bone surgery. These implants are made of skeletal material obtained from animals (Merkx et al., 2003), in most cases from equine, bovine or porcine bones. Animal material is processed by means of thermal treatment in order to deplete it completely of its organic components (Barakat et al., 2009). As a result, implants lose their immunogenic properties and become neutral to hosts (Liu et al., 2008). Therefore, ready to use preparations for bone replacement (Bio-Oss®, Endobone®) are most frequently available in deproteinized forms (DBBM) (Accorsi-Mendonça et al., 2008). Due to their osteoconductive properties they can serve as an inactive scaffold or platform for the maturation of bone cells present within the defect. They are used in orthopedics, dental and maxillofacial surgery, as well as in periodontology and implantology, etc. (Baldini et al., 2011; Cao et al., 2009; Jian et al., 2008; Merkx et al., 2003; Precheur, 2007; von Wattenwyl et al., 2011). The limited possibilities of modulating the resorption time of such preparations during skeletal tissue reconstruction, however, can be related to the poorer quality of bone at the site of their application.

An alternative solution, eliminating the potential complications associated with the application of materials of autogenous, allogenic or xenogenic origin, is the use of alloplastic implants for the purpose of bone replacement. Such implants can be synthesized from both natural and synthetic materials (Bohner, 2010; Giannoudis et al., 2005). Bioresorbable ceramic based on calcium phosphate plays a distinct role amongst novel synthetic materials used for bone replacement (Barradas et al., 2011). Hydroxyapatite (HAp) is the principal representative of this group, with the widest application in reconstructive surgery. Due to its calcium phosphate content and natural occurrence as an inorganic substance in bones and teeth, hydroxyapatite is characterized by the highest biocompatibility and bioactivity of all currently known implant materials. Additionally, due to the osteoconductive properties of hydroxyapatite, and (to a lesser extent) its osteoinductive properties, hydroxyapatite-based implants can bind directly to bone. Numerous clinical trials, supported by the results of histological observations, have confirmed complete biotolerance to hydroxyapatite ceramic, as well as its positive effects on the process of bone healing and reconstruction. Additionally, hydroxyapatite ceramic can initiate and stimulate various processes that are associated with bone formation (Bellucci et al., 2011; Ravarian et al., 2010; Yuan et al., 2001). Contact between bioactive ceramic and living skeletal tissue induces osteogenesis. As a result, an intermediate binding layer is formed between the living tissue and the implant, serving as a kind of biological glue. The structural similarity of calcium phosphate-based ceramic and the natural mineral components of bone is crucial for infiltration of the implant by the skeletal tissue of the host. This supports the intra-tissue application of hydroxyapatite-based implants whenever long-term remodeling of bone is required. Beta-

tricalcium phosphate (betaTCP, beta$Ca_3(PO_4)_2$) is another calcium phosphate that has been used successfully in bone substitution. Its mineralogical analogue is whitlockite (TCP) (Barradas et al., 2011). Similar to HAp, TCP is characterized by high biocompatibility. In comparison to hydroxyapatite materials, it has a higher solubility *in vitro* and a resultant higher susceptibility to resorption and biodegradation in the environment of the living organism (Bohner, 2010; Henkel et al., 2006). TCP is considered an osteoinductive material, which stimulates the processes of bone reconstruction (Wang et al., 2009). Many studies, mostly dealing with the gradual, controlled resorption rate of calcium phosphate ceramic, resulted in the design of the second polymorphic variant of TCP, namely αTCP (Zima et al., 2010). Similar to beta-TCP, it is formed as a result of the non-stoichiometric heating of HAp with a well-defined temperature and defined kinetics of thermal processing. Compared to beta-TCP, αTCP has an approximately five-fold higher susceptibility to resorption in living tissues, along with higher biocompatibility (Oonishi et al., 1999). The high degree of osteointegration of αTCP-based bioceramic is plausibly the result of the higher solubility of $\alpha Ca_3(PO_4)_2$ than of HAp or βTCP. Delivered within the ceramic, calcium and phosphate ions constitute the material for synthesizing the layer composed of non-stoichiometric hydroxyapatite that binds the implant to bone (Kon et al., 1995). Some authors suggest that αTCP can be cytotoxic, probably due to pH changes that are induced *in vitro* (Santos et al., 2002). These suggestions, however, were not confirmed during *in vivo* studies, and αTCP is included in many commercially available bone cements. Since the 1990s, biphasic HAp-βTCP ceramic (BCP biphasic calcium phosphate) has also been used in the reconstruction of skeletal defects (Deculsi, 1998, Deculsi et al., 2003; Fellah et al., 2008; Schwarz et al., 2007).

Bio-glass and apatite-wollastonite glass-ceramic also play an important role amongst the bioactive materials used in the processes of bone synthesis. The biological activity of glass and glass-derived crystalline materials (glass-ceramic materials) is mostly exploited for the manufacture of surface-active implants or implants that can be resorbed in the human body (Giannoudis et al., 2005). The composition of surface-active materials is selected in order to enable interactions between the physiological environment and certain components of the implant. As a result, living tissue is bound to the implant surface. Resorbable glass is characterized by its high content of chemical elements involved in metabolic processes of the human body. In both cases, living tissues can infiltrate the implant and bind it directly to the bone. These processes result not only from the chemical composition of the implants but also from the specific nature of the contained glass substance. The binding abilities of bioactive glass and glass-ceramic implants to skeletal tissue have been the subject of many studies. These studies confirmed the usefulness of such materials in tissue engineering, where they can be used in cell culture (Ferreira, 2007; Xynos et al., 2000). Their application in reconstructive surgery is reflected by their ability to stimulate and supporting bone reconstruction. In view of their confirmed ability to directly bind to skeletal tissue, they have been used successfully in various stomatological disciplines, including implantology, dental surgery and periodontology. Moreover, modern surface engineering has allowed the coating of metal implants with bioactive glass. Such coatings either protect surfaces of metal alloys against corrosion and wear, or stimulate the processes of bone formation in their surroundings. Additionally, resorbable glass can be used as a drug carrier, providing prolonged release of an active substance. Furthermore, some attempts have been made to combine various materials with each other to manufacture glass-containing bioactive composites, used as the components of binders, among others (Bellucci et al., 2011). These

experiments were aimed at obtaining biomaterials with better durability parameters and optimal biological characteristics. Various types of bio-glass and glass-ceramics may differ in terms of their biological properties, depending on the technique for their synthesis (Bellucci et al., 2011; Yuan et al. 2001). Amongst various methods of synthesis, the advantages of the chemical sol-gel method are worth noting. This technique enables material whose biological activity is greater than products manufactured using other processing methods to be obtained (Ravarian et al., 2010). Moreover, the sol-gel method does not require high temperature processing. Additionally, this technique allows the production of material with a strictly defined texture and parameters. Due to the possibility of manufacturing porous forms, bio-glass and glass-derived crystalline materials are morphologically similar to bone; this facilitates their infiltration by bone cells at the implantation site. Additionally, the porous structure of the implant enables the supply of fluids and nutrients required for growth to the newly formed bone, as well as the elimination of metabolites (Yuan et al., 2001). Finally, the resorption rate of the implant material is also determined by the degree of its porosity.

In view of the complexity of the biological environment at the implantation site, one principle problem of biomaterial engineering pertains to issues associated with the biodegradation and bioresorption of implanted biomaterials. Determination of degradation time and rate, and the kinetics of this process in the human body, constitute a significant challenge in the design of new implant materials (including bioceramic) used for the purposes of skeletal tissue substitution (Daculsi et al., 2003; Giannoudis et al., 2005). The controlled degradation rate of the implant along with the associated reconstruction of skeletal tissue should result in the formation of bone tissue resembling its natural structure as closely as possible, both at the biological and physico-mechanical levels. One of many methods allowing for the controlled biodegradation of bone replacement materials is the design of implants made of various composites or mixtures. Combining two or more different materials results in the manufacture of an absolutely new composite biomaterial, which is frequently superior in terms of biological and mechanical properties. Due to its specific properties, bioceramic is very frequently used as a basic component of ceramic-ceramic, metal-ceramic and polymer-ceramic systems (Thomas et al., 2005). Hydroxyapatite is very frequently included in bone composites, mostly due to its chemical similarity to the natural components of bone. Some studies have confirmed the positive effects of hydroxyapatite used in combination with metals, ceramic or polymers (Abu Bakar et al., 2003; Bellucci et al., 2011; Choi et al., 2004; Daculsi et al., 2003). The results of research on HAp-containing composites based on resorbable polymers, mostly polylactide (PLA), polyglycolide (PGA), co-polymer of glycolide and lactide (PLGA) or collagen [Cieślik et al., Nagata et al., 2005], seem particularly interesting. These studies confirmed the possible application of such composites as binding and reconstructive elements in reconstructive surgery, as culture media in tissue and genetic engineering, and as drug carriers (Wei & Ma, 2004; Nagata et al., 2003). Although hydroxyapatite is characterized by high biocompatibility, its reactivity with living skeletal tissue is relatively low. In view of these findings, attempts to design composites that combine this biomaterial with markedly more biologically active bio-glass propose an interesting solution. Such a composite can stimulate osteogenesis, leading to the rapid formation of new skeletal tissue around the implant (Yuan et al., 2001; Ravarian et al., 2010). Biological tests of SiO_2-CaO-Mg/natural HAp (bovine bone) composite obtained by means of thermal plasma processing have confirmed its lack of

toxicity. Moreover, the glass-ceramic contained in this composite was confirmed to stimulate the growth and proliferation of human fibroblasts (Yoganand et al., 2010). Attempts at bone replacement with materials obtained by combining autogenous bone and deproteinized bovine bone constitute another example of the potential optimization of biological conditions for new skeletal tissue growth within a skeletal defect. The inclusion of autogenous material with osteoinductive properties in such composites results in the enhanced formation of better quality bone (Kim et al., 2009; Pripatnanont et al., 2009; Thorwarth et al., 2006; Thuaksuban et al., 2010). *In vitro* cellular studies have confirmed that allogenic materials of human origin (demineralized bone matrix, deproteinized bone) may also have some osteoinductive activity. This activity was confirmed by an increase in alkaline phosphatase (ALP), osteocalcin (OC) and Ca^{2+} concentrations observed in human bone marrow stromal osteoprogenitor cells (hBMSCs) cultured for three weeks in medium based on human bone components (Zhang et al., 2009).

The increasing demand for bone replacement materials stimulated us to design original composite materials for use in the regeneration of skeletal defects, characterized by both osteoinductive and osteoconductive properties. In designing such composites, we have used well-described biomaterials that have been applied successfully to skeletal defect regeneration, namely bio-glass (BG) and tricalcium phosphate (TCP). Lyophilized human bone obtained from a tissue bank served as a base for designing three types of mixtures: 1) human bone/bio-glass; 2) human bone/TCP; and 3) human bone/bio-glass/TCP. Such variants of material combinations enabled us to analyze the effects of particular components on the process of bone formation, and specifically on its dynamics and on the quality of newly formed bone. Also, the selection of the components included among the analyzed materials (mixtures) was not accidental. We have assumed that both bio-glass and tricalcium phosphate will activate and stimulate osteoblasts to dynamically grow on a biological scaffold of lyophilized human bone, thereby providing optimal biological conditions for the formation of full value bone.

2. Material

The materials used in the study included lyophilized, deproteinized human bone (B) – group B, and its mixtures with: 1) bio-glass (BG) in a proportion of 80:20% weight ratio (B:BG) – group B+BG; 2) tricalcium phosphate (TCP) in a proportion of 80:20% weight ratio (B:TCP) – group B+TCP; 3) bio-glass and tricalcium phosphate in a proportion of 70:15:15% weight ratio (B:BG:TCP) – group B+BG+TCP. The deproteinized human bone and all other components used in the mixtures were in a granulated form with diameters ranging from 0.3 to 0.5 mm.

Human bone used in this study was obtained from the Tissue Bank of the Regional Center of Blood Donation and Treatment in Katowice (Poland). It was cancellous bone subjected to lyophilization, deep freezing and irradiation sterilization with a dose of 35 kGy.

The bio-glass was made from the $CaO\text{-}SiO_2\text{-}P_2O_5$ system with the use of the sol-gel technology, in the laboratory of the Department of Glass and Amorphous Coatings at the AGH Science and Technology University in Cracow, Poland. Its high-calcium A2 variety was used (54% mol. CaO) with a density of 2.9082 g/cm^3, a dominating glassy phase and the beginnings of apatite crystallization. The thermal treatment of the bio-glass was performed

at a temperature of 800˚C, and its specific surface area (calculated by BET method) amounted to 57.8166 m^2/g.

Resorbable, monophasic βTCP ceramic – a salt of trialkaline orthophosphoric acid $Ca_3(PO_4)_2$ – was synthesized from powdered components obtained by means of wet synthesis in the Bioceramic Laboratory of the Department of Ceramic and Fire Resistant Material Technology at the AGH Science and Technology University in Cracow, Poland (Ślósarczyk & Paszkiewicz, 2005; Zima at al., 2010). The reagents included CaO (obtained by means of calcination of $Ca(OH)_2$ – pure for analysis; MERCK, Poland), and H_3PO_4 (pure for analysis; POCH, Poland).

3. *In vivo* animal experiments

The study was carried out on a group of 48 guinea pigs, with an equal number of both sexes, and weights ranging from 500 to 600 grams. The animals were divided randomly into four groups, which corresponded to 12 animals for each studied composite material (6 males and 6 females). The animal experiments were performed on the 7th, 14th, and 21st days of the study, as well as after the 4th, 8th and 12th experimental weeks. Two guinea pigs (one male and one female) were examined in each experiment. All animal surgical procedures were performed at the Central Experimental Animal Farm at the Medical University of Silesia and were granted permission by the university's Bioethical Board for Experimental Animals.

Before starting any surgical procedures, the animals received general anesthesia with thiopental (0.4 g/kg b.w.). Bone defects (6 mm in diameter and 3 mm in depth) were formed bilaterally on the external surface of the mandibular trunk, 2 mm below its lower edge (between the radices of the incisive and molar teeth) with the aid of a rosette burr placed in the straight hand-piece of a dental machine (Fig.1a). Depending on the experimental group, bone defects on the right side of the mandible were filled with: 1) a preparation of deproteinized human bone (group B), 2) a mixture of deproteinized human bone and bio-glass (group B+BG), 3) a mixture of deproteinized human bone and tricalcium phosphate (group B+TCP), or 4) a mixture of deproteinized human bone with bio-glass and tricalcium phosphate (group B+BG+TCP). Before implantation into the mandibular bone defect, each material was mixed with the animal's blood obtained from the surgical wound (Fig. 1b) in a

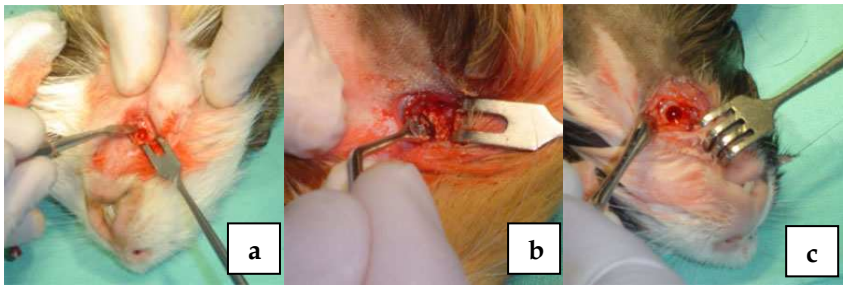

Fig. 1. Bone defect in the mandibular trunk of the experimental animal: a) defect prepared for filling with implant based on deproteinized human bone; b) defect filled with the mixture of deproteinized human bone and bio-glass with animal's blood; c) control defect filled with postoperatively clotted blood

proportion of 25:75% weight ratio (examined material to blood). Blood served as a binder, supplying the implanted material with organic components. Additionally, it prevented the displacement of the implanted granules from within the bone defect, and facilitated their insertion. The defect on the left side of the mandible was left to fill postoperatively with clotted blood and undergo spontaneous healing (Fig.1c), and was considered a control to the right mandibular defect in each animal (control group). The bilateral wounds were closed in multiple layers with Dexon 4.0 sutures.

4. Methods of examination

On each examination day, all guinea pigs were clinically evaluated for surgical wound healing and general condition. Additionally, radiographs were taken in order to assess the regeneration of mandibular bone defects. Newly formed skeletal tissue in the defects was also analyzed quantitatively and qualitatively in terms of bone mineral density at the implantation site (computed tomography and radiographic densitometry). Following euthanasia with Morbital (sodium pentobarbital 133.3 mg/mL and pentobarbital 26.7 mg/mL, 1-2 mL/kg b.w.), the operated area and surrounding tissues were examined macroscopically. Moreover, tissue specimens from the euthanized animals were subjected to histopathologic analysis of the skeletal tissue and bone marrow at the implantation site and at its periphery, including the healing rate of the skeletal tissue and the soft and hard tissue reactions to the implanted material. Histopathologic analysis also included organs involved in detoxification of the body (i.e. liver and kidneys).

Radiographs of the mandibular trunk with the sites of the bone defects were taken with a Heliodent type MD/D – 3195 nr 051692 apparatus (SIEMENS), and AGFA DENTUS M2 CONFORT films for axial pictures (75 mm x 65mm), using the following exposure conditions: 0.16 s, 7 mA and 60 kV.

The tissue specimens taken for the histopathologic examinations were preserved in a 10% solution of buffered formalin. The osseous tissue was decalcified either in a 10% solution of disodium versenate, or electrolytically in Romeis liquid (80 mL of hydrochloric acid + 100 mL of formic acid, diluted to make 1000 mL with water) using PW23 bone decalcifier and an electric current of 0.5A. Next, all the tissues were routinely processed in Technicon's Duo autotechnicon using the sequence of 96% alcohol, acetone and xylene. They were then embedded in paraplast. The obtained cubes were then shaved on a Microm HM335E rotating microtome. The shavings (4-6 microns in thickness) were put onto basic slides, deparaffinized, and stained with hematoxylin and eosin (H&E). They were subsequently mounted with Canada balsam. Histologic slides were analyzed under an Olympus BX50 light microscope equipped with a set for optical (Olympus SC35) and digital microphotography (Olympus Canmedia C-5050 Zoom), at 40 to 400 x magnification. Additionally, the slides were consulted by other histologists using a dual-head Nikon Labophot-2 microscope.

Bone mineral density (BMD) was determined by means of dual-energy X-ray absorptiometry (DXA) with a DPX-L densitometer (LUNAR Radiation Corporation, Madison, USA) using Small Animal Appendicular scanning. Total bone mineral density (BMD; g/cm^2) was determined on the basis of examination of the entire area of the transverse cross-section of the bone defect (28.26 mm^2), analyzed as 0.5 mm^2 to 3 mm^2 sections. One hundred and twenty

BMD measurements were taken in each group (corresponding to 20 measurements per experimental day). In most cases, reproducible results were not included in further analysis; only unique values and the most frequent reproducible values were analyzed, which corresponded to 10 BMD measurements for each day of examination. Additionally, the BMD of the normal mandibular trunk of the guinea pig was determined for the purpose of comparative analysis. Based on 10 consecutive measurements, this value was estimated at 0.51 ± 0.001 g/cm^2. During the measurements, the densitometer was regularly calibrated and controlled according to the manufacturer's recommendations. Both DXA measurements and BMD result analysis were performed by the same investigator.

Additionally, computed tomography (CT) was used to determine the bone mineral density, expressed in Hounsfield units (HU). These measurements were taken using a Somatom Emotion 6 scanner (Siemens; exposure parameters: 13.4 s, 14 mA, 130 kV). Transverse cross-sections of the mandible were visualized in 2 mm slices. Then, cross-sections including the area of the bone defect were selected and analyzed using Volume Viewer software. In each experimental group, six measurements were taken for each examination day. Additionally, six measurements of the normal mandible were taken for the purpose of comparative analysis. Based on these measurements, the normal bone mineral density was determined to be 1218 ± 15.2 HU.

The results of bone density are presented as mean values ± standard deviation. Variables distribution was evaluated by the Shapiro-Wilk test. Homogeneity of variance was assessed by the Levene test. ANOVA for repeated measurements with contrasts analysis were done to assess time and preparation of deproteinized human bone type interaction. The Mauchley test was done to check sphericity. Differences were considered to be statistically significant at $p<0.05$. All calculations were performed using the commercially available statistical package Statistica 9.0.

5. Results

5.1 Clinical observations

Throughout the entire study period, no complications in surgical wound healing were observed in animals of any experimental group. The guinea pigs were calm, which suggested a lack of pain. The animals ate and drank water normally, and neither scraped against the cage nor scratched their wounds during the entire postoperative period. Also, wound dehiscence was not observed in any of the groups.

Tissue edema over the surgical skin wounds resolved 3 to 5 days following surgery and was replaced by protrusions of the tissue. There were no signs of excessive fluid accumulation around the wound or of hematoma formation, but in some animals skin redness was observed around the stitches. In most animals, tissue protrusions persisted until the 21st day after surgery. The stitches were removed 10 to 14 days after surgery. Over the entire study period, the animals gained weight gradually (in a statistically insignificant manner).

5.2 Macroscopic examination

Up to 14th experimental day, the sites of the implanted bone defects were clearly distinguishable from the surrounding tissues as clear, oval protrusions covered with delicate

tissue, which could be compressed elastically. Additionally, clearly distinguishable white granulation was visible throughout the superficial tissue in animals of the B+BG and B+BG+TCP groups. Probably, these granules corresponded to the bio-glass particles included in the material implanted in these groups. In the control group, the site of the bone defect was visible as a clear protrusion up to the 7th experimental day. On the next day of examination (the 14th day), however, the site was covered with a tissue whose coloration was darker in comparison to the surrounding tissues.

After the 3rd experimental week, the protrusion visible over the implantation site in groups B+BG, B+TCP and B+BG+TCP was markedly smaller in size, and covered with a hard tissue of more compact texture. Coloration of the tissues covering the implantation site still differed from the color of normal bone. In group BG, white granulation was still visible throughout the superficial tissue. On the 21st day after surgery, the coloration of the bone defect implanted with deproteinized human bone (group B) resembled the color of the surrounding tissues more closely than in previous periods. In both group B and in the control group, clearly distinguishable small areas in the form of a dark-colored spot were visible within the defects. Additionally, tissue protrusion observed over the defects in the control group increased in size when compared to previous periods.

Four weeks following implantation, the area of the bone defect in group B+BG was slightly smaller in size but still clearly distinguishable and differed in color from the surrounding tissues. Similar changes were observed in the B+TCP group; the implantation site in this group was concave, but still appeared hard when compressed. The tissue visible over the implantation site in group B+BG+TCP resembled the surrounding normal tissues the most closely when compared to the other groups. In group BG, white granulation was still visible throughout the superficial tissue covering the bone defect. In the control group, on the other hand, a large protrusion was still visible over the implantation site, with a small dark-colored spot at its center.

After the 8th and 12th weeks of experiment, the implantation sites of the group B animals were still clearly distinguishable on macroscopic examination; they were protruding and differed in color from the surrounding tissues. Protrusions over the implantation sites were also visible in group B+BG, but only up to the 8th week of the study. After this time, the implantation site was hardly distinguishable from the normal tissues, and only the presence of granulation, which was hardly visible throughout the superficial tissue, enabled its visual identification. In group B+BG+TCP, the implantation site could also only be localized due to the subtle appearance of white granulation as early as after 8 weeks of the experiment. In group B+TCP, no concavity was observed over the implantation site beginning from the 8th week of the study, and the tissue covering the defect only slightly differed in color from the surrounding normal bone. After 12 weeks of observation, the tissue over the bone defects in this group had an identical appearance to the surrounding tissues. On the last examination day, the site of the bone defect was distinguishable only in the control group. Although the implantation site was covered with hard tissue, minute concavities and dark spots were still visible on its surface.

5.3 Radiological examinations

Material-related differences in the rates of new skeletal tissue formation were revealed as early as after the 7th day of the study. In group B, spherical translucencies with regular

edges were observed on radiographic images, with a size corresponding to the size of the bone defect. The initial process of bone reconstruction, manifested by a foggy appearance of the implantation site, was observed no earlier than after the second experimental week (Fig. 2a). At that same time point, initial signs of bone formation were also observed on radiographic images taken in group B+BG+TCP (Fig. 5a), while in group B+BG this phenomenon was already visible after 7 days (Fig. 3a). Irregular translucencies at the implantation site were seen in this group, but a small shadow was observed in the central zone, whose area and intensity increased with time. Radiologic findings suggested that the beginning of new tissue formation was most delayed in group B+TCP (Fig. 4a) and in the controls (Fig. 6a). In these groups, a distinct shadow was observed no earlier than after the 3rd week of the experiment; this shadow was larger and more intense in B+TCP group.

After the 4th week of the study, radiographic images taken in group B revealed the nearly complete formation of new skeletal tissue. At this point in time, indistinct translucencies were seen only at the periphery of the skeletal defect, suggesting osteogenesis was ongoing in this area. After 8 weeks of the experiment, bone reconstruction was complete in this group. The whole defect was excessively shadowed, suggesting that tissue with greater mineralization was present in this area when compared to normal bone (Fig. 2b). As with group B, in group B+TCP the mineralization of the implantation site was complete after the 8th week of the study, as suggested by a fully shadowed area of the bone defect visible on radiographic images (Fig. 4b). At the same time, a small translucency was visible in the superior-medial aspect of the bone defect in group B+BG. In this group, the process of bone formation was completed no earlier than after the 12th week of the experiment. This was confirmed by the excessive mineralization of skeletal tissue, manifested radiographically as a distinct shadow at the implantation site (Fig. 3b). In the B+BG+TCP group, a homogenous shadow was visible at the implantation site as early as after the 8th week of the experiment, and an incomplete process of skeletal tissue regeneration was suggested only by the presence of spotted translucencies. However, the site of the bone defect could not be distinguished from the surrounding tissues until at least the 12th week of the study (Fig. 5b). In the control group, the process of bone formation was markedly delayed, and after the 8th week of the study a distinct, longitudinal translucency could still be seen at the site of the bone defect. Moreover, non-calcified areas were still visible on the last examination day despite newly formed skeletal tissue present within the entire area of the bone defect (Fig. 6b).

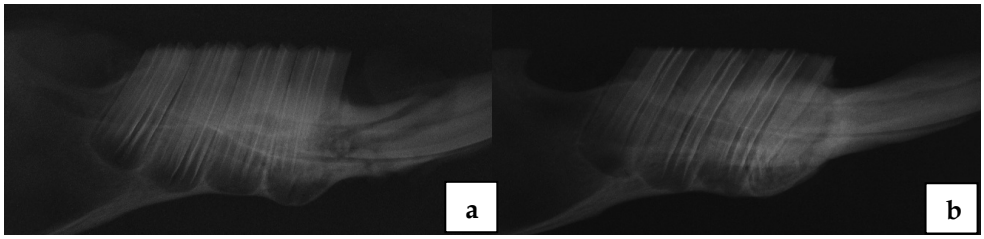

Fig. 2. Radiographic images of the mandible in experimental animals. Bone defect healing in the presence of deproteinized human bone: a) 14th day of the study; b) 8th week of the study

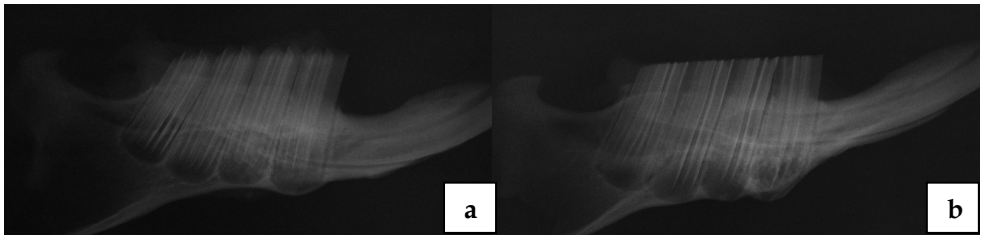

Fig. 3. Radiographic images of the mandible in experimental animals. Bone defect healing in the presence of the mixture of deproteinized human bone with bio-glass: a) 7th day of the study; b) 12th week of the study

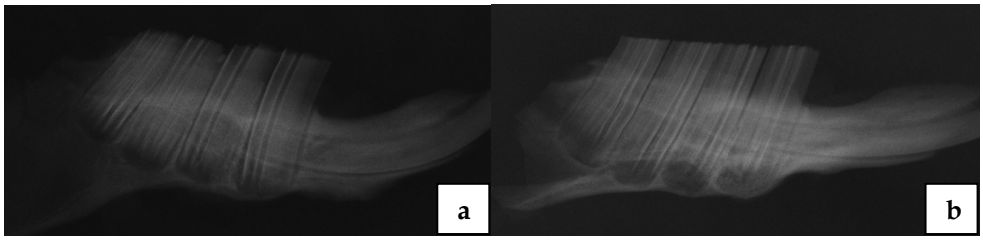

Fig. 4. Radiographic images of the mandible in experimental animals. Bone defect healing in the presence of the mixture of deproteinized human bone with tricalcium phosphate: a) 21st day of the study; b) 8th week of the study

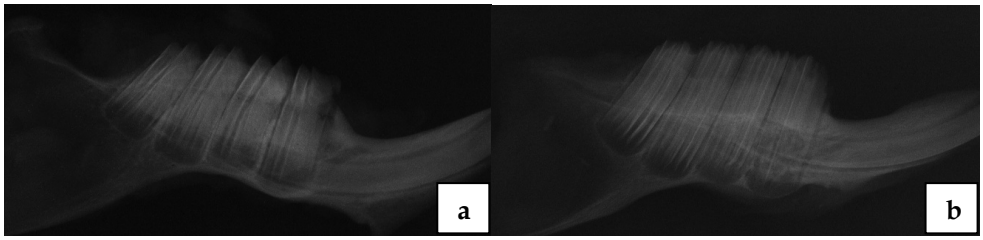

Fig. 5. Radiographic images of the mandible in experimental animals. Bone defect healing in the presence of the mixture of deproteinized human bone with bio-glass and tricalcium phosphate: a) 14th day of the study; b) 12th week of the study

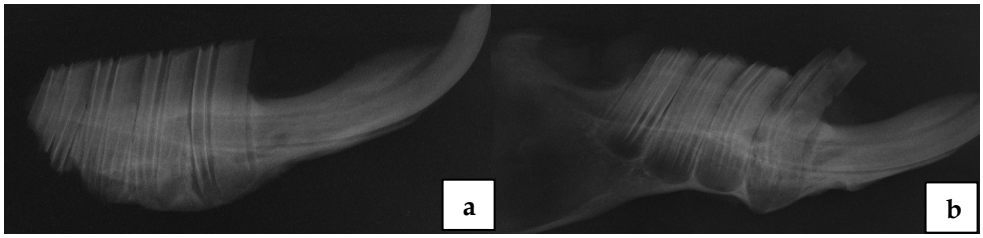

Fig. 6. Radiographic images of the mandible in experimental animals. Bone defect healing on the basis of clotted blood: a) 21st day of the study; b) 12th week of the study

5.4 Bone Mineral Density

5.4.1 Radiographic densitometry

A gradual increase in BMD was observed in all experimental groups and in the controls. The highest BMD value was observed after the 8th week of the study in bone defects implanted with B+TCP (0.40±0.05 g/cm^2) and B+BG+TCP (0.39±0.05 g/cm^2) (Table 1). However, these values were still lower than the normal BMD of the mandibular trunk determined in guinea pigs (0.51± 0.001 g/cm^2).

	BMD [g/cm^2]					
Group	**1st week**	**2nd week**	**3th week**	**4th week**	**8th week**	**12th week**
B	0.25 ± 0.01	0.27 ± 0.01	0.28 ± 0.01	0.33 ± 0.02	0.35 ± 0.03	0.35 ± 0.03
B+BG	0.27 ± 0.02	0.30 ± 0.03	0.30 ± 0.03	0.31 ± 0.02	0.31 ± 0.03	0.33 ± 0.01
B+TCP	0.22 ± 0.03	0.24 ± 0.03	0.33 ± 0.01	0.32 ± 0.04	0.40 ± 0.05	0.36 ± 0.02
B+BG+TCP	0.23 ± 0.03	0.28 ± 0.02	0.32 ± 0.03	0.35 ± 0.04	0.39 ± 0.05	0.38 ± 0.02
Control	0.24 ± 0.01	0.25 ± 0.01	0.22 ± 0.02	0.34 ± 0.01	0.33 ± 0.04	0.32 ± 0.02

Table 1. Bone mineral density (BMD) of skeletal defects implanted with various materials and in control defects determined radiographically at various time points in the study

The most regular increase in BMD was observed in defects implanted with B+BG+TCP, followed by B and B+BG. Some irregularities in the time profiles of BMD changes were noted, however, in animals of group B+TCP and in the controls, suggesting inhomogeneous formation of new skeletal tissue (Fig. 7).

Additionally, statistical analysis revealed intergroup differences in the time profiles of BMD changes. The most pronounced differences were observed between groups B and B+BG – 0.98, followed by B+BG vs. B+TCP – 0.79, and B vs. B+TCP – 0.78. Slight differences in the time profiles were noted between the B+BG+TCP group and other material groups, and no significant differences were observed when experimental groups were compared to the control group (Table 2).

	Profile comparison (p-values)			
Group	**Control**	**B**	**B+BG**	**B+TCP**
B	**<0.05**	–	–	–
B+BG	**<0.05**	0.98	–	–
B+TCP	**<0.05**	0.78	0.79	–
B+BG+TCP	**<0.01**	0.20	0.21	0.32

Table 2. The p-values for comparison of bone mineral density (BMD) changes in time (profiles) between the tested material and control groups

Moreover, a relative increase in BMD between the 1st and 12th experimental weeks was calculated for each group (Table 3). The highest relative increase in BMD was observed in bone defects in group B+BG+TCP (25.49) but the increase in the B+TCP group was only slightly lower (24.14). The lowest relative increase in BMD between the 1st and 12th

experimental weeks was observed in animals of group B+BG (9.98); the time plot of BMD changes in this group was closest to a vertical line.

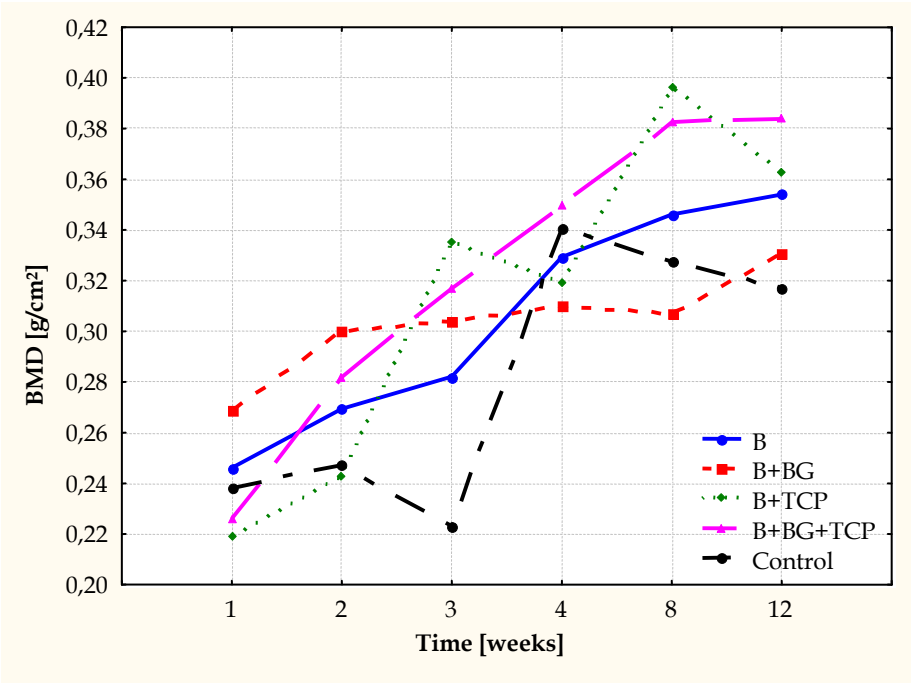

Fig. 7. Time profile of changes in bone mineral density (BMD) determined radiographically in bone defects implanted with various materials and in control defects

Due to non-sphericity (Mauchley test: 0.42; $p<0.001$) only multivariable tests were used. We confirmed that there were statistically significant changes in BMD with time ($F = 894.17$; $p<0.001$). Moreover, the interaction between time and the type of material used (group) was also statistically significant ($F = 35.59$; $p<0.001$).

	12th vs. 1st week	
Group	|t|	p
B	17.11	**<0.001**
B+BG	9.98	**<0.001**
B+TCP	24.14	**<0.001**
B+BG+TCP	25.49	**<0.001**
Control	13.58	**<0.001**

Table 3. Comparison of bone mineral density (BMD) values between the 12th and 1st weeks with regard to the tested material and control groups

Finally, statistical analysis revealed several significant intergroup differences in BMD values determined in experimental weeks 1 and 12 (Table 4). In the earlier period, the most

pronounced difference was observed between groups B+BG and B+TCP (4.33), while the lowest difference pertained to groups B+TCP and B+BG+TCP. After 12 weeks of the experiment, the most pronounced difference in BMD of the bone defect was noted between the control group and the B+BG+TCP group, while the difference between the B and B+TCP groups was the lowest.

	1st week		12th week	
Groups	|t|	P	|t|	p
B vs. Control	0.70	0.48	3.63	**<0.001**
B+BG vs. Control	2.48	**<0.05**	1.41	0.17
B+TCP vs. Control	1.85	0.07	4.54	**<0.05**
B+BG+TCP vs. Control	1.27	0.21	6.40	**<0.001**
B vs. B+BG	1.78	0.08	2.22	**<0.05**
B vs. B+TCP	2.55	**<0.05**	0.91	0.37
B vs. B+BG+TCP	1.98	0.05	2.78	**<0.01**
B+BG vs. B+TCP	4.33	**<0.001**	3.13	**<0.01**
B+BG vs. B+BG+TCP	3.75	**<0.001**	4.99	**<0.001**
B+TCP vs. B+BG+TCP	0.57	0.57	1.87	0.07

Table 4. Comparison of bone mineral density (BMD) values in the 1st and 12th weeks between the tested material and control groups

We have also observed statistically significant differences in the growth of BMD with time between the analyzed groups ($F=8.15$; $p<0.001$). The smallest changes in BMD were yielded by B+BG (0.06±0.01), then the control group (0.08±0.01) and B (0.11±0.02). The largest changes were observed for B+TCP (0.14±0.01) and B+BG+TCP (0.16±0.01). For all paired comparisons, statistically significant differences were noted ($p<0.01$).

5.4.2 Computed tomography

Table 5 summarizes the values of bone density in the experimental groups and in the controls as determined by CT. A gradual increase in the density of healing bone defects was observed in all studied groups. After 12 weeks of the experiment, the highest values of CT bone density were observed in the B+BG (1014.8±53.9 HU) and B+BG+TCP (941.2±28.9 HU) groups, while the lowest values were noted in the controls (812.3±21.8 HU). However, the highest determined values of CT bone density were still lower compared to the bone density of the normal mandible (1218 ± 15.2 HU).

	CT Bone Density [HU]					
Group	**1st week**	**2nd week**	**3th week**	**4th week**	**8th week**	**12th week**
B	647.7 ± 79.1	784.0 ± 82.3	863.2 ± 13.3	763.8 ± 136.1	954.3 ± 56.3	902.8 ± 13.5
B+BG	597.2 ± 48.8	730.5 ± 9.8	814.3 ± 38.1	822.5 ± 99.8	933.3 ± 22.0	1014.8 ± 53.9
B+TCP	410.3 ± 34.0	468.2 ± 59.1	606.7 ± 41.8	804.0 ± 51.7	826.3 ± 39.3	879.2 ± 24.6
B+BG+TCP	454.7 ± 17.1	526.3 ± 35.6	523.2 ± 27.7	725.7 ± 36.3	923.7 ± 31.8	941.2 ± 28.9
Control	256.0 ± 20.4	510.3 ± 28.7	539.0 ± 38.3	597.8 ± 35.3	681.8 ± 19.4	812.3 ± 21.8

Table 5. CT bone density (expressed in Hounsfield units, HU) in bone defects implanted with various materials and in control defects at various time points in the study

The most homogeneous increase in CT bone density values was observed in groups B+BG and B+TCP, and in the controls. Some irregularities in the time profile of bone density were, by contrast, noted in animals of the B and B+BG+TCP groups (Fig. 8).

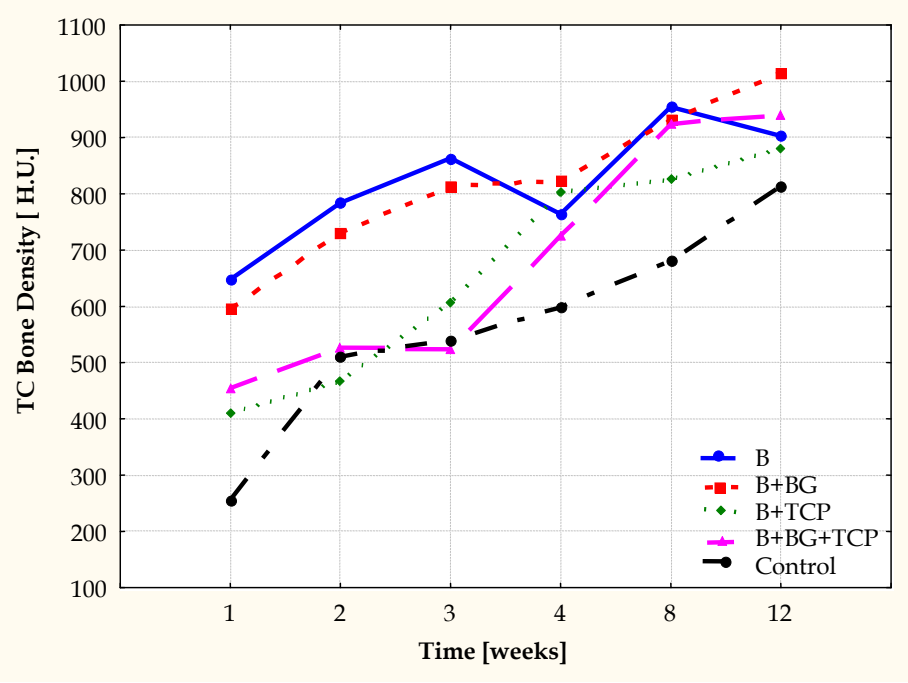

Fig. 8. Time profile of changes in CT bone density (expressed in Hounsfield units, HU) in bone defects implanted with various materials and in control defects

Due to non-sphericity (Mauchley test: 0.0030; $p<0.001$) only multivariable tests were used. We confirmed that there were statistically significant changes in Hounsfield Units with time ($F = 1244.88$; $p<0.001$). Moreover, the interaction between time and the type of material used (group) was also statistically significant ($F = 65.35$; $p<0.001$).

When the time profiles of CT bone density changes were compared between the studied groups, the only significant differences observed were between groups B and B+BG – 0.86, and B+TCP and B+BG+TCP – 0.30 (Table 6).

Profile comparison (p-values)				
Group	**Control**	**B**	**B+BG**	**B+TCP**
B	**<0.001**	–	–	–
B+BG	**<0.001**	0.86	–	–
B+TCP	**<0.001**	**<0.001**	**<0.001**	–
B+BG+TCP	**<0.001**	**<0.001**	**<0.001**	0.30

Table 6. The p-values for comparison of CT bone density (expressed in Hounsfield units, HU) with changes in time (profiles) between the tested material and control groups

The most evident intragroup differences in CT bone density determined in the 1st and 12th experimental weeks were observed in the control group (29.77), but the differences were only slightly less pronounced in groups B+TCP (24.10) and B+BG+TCP (22.94). The least evident differences between the two analyzed time points were noted in the B (10.67) and B+BG (16.77) groups (Table 7).

	12th vs. 1st week	
Group	|t|	p
B	10.67	**<0.001**
B+BG	16.77	**<0.001**
B+TCP	24.10	**<0.001**
B+BG+TCP	22.94	**<0.001**
Control	29.77	**<0.001**

Table 7. Comparison of CT bone density values (expressed in Hounsfield units, HU) between the 12th and 1st weeks with regard to the tested material and control groups

After seven days of the experiment, the most pronounced intergroup differences in CT bone density were observed between the control group and groups B and BG. The least pronounced intergroup differences noted in this period pertained to groups B and B+BG. After 12 weeks of the study, the most evident intergroup differences in CT bone density were again observed between the controls and group B+BG, while the lowest differences were noted between groups B and B+TCP.

	1st week		**12th week**	
Groups	|t|	p	|t|	p
B vs. Control	16.63	**<0.001**	4.91	**<0.001**
B+BG vs. Control	15.23	**<0.001**	10.29	**<0.001**
B+TCP vs. Control	8.48	**<0.001**	3.67	**<0.05**
B+BG+TCP vs. Control	10.36	**<0.001**	6.83	**<0.001**
B vs. B+BG	1.56	0.1325	6.01	**<0.001**
B vs. B+TCP	9.11	**<0.001**	1.39	0.1779
B vs. B+BG+TCP	7.00	**<0.001**	2.14	**<0.05**
B+BG vs. B+TCP	7.55	**<0.001**	7.40	**<0.001**
B+BG vs. B+BG+TCP	5.44	**<0.001**	3.87	**<0.001**
B+TCP vs. B+BG+TCP	2.11	**<0.05**	3.53	**<0.01**

Table 8. Comparison of CT bone density (expressed in Hounsfield units, HU) values in the 1st and 12th weeks between tested material and control groups

We have also observed statistically significant intergroup differences in the relative increase in CT bone density (expressed in Hounsfield units, HU) ($F = 39.22$; $p<0.001$). The smallest changes in CT bone density were yielded by group B (255.2±67.6). Larger changes were observed for B+BG (417.7±25.7), B+TCP (468.8±43.3) and B+BG+TCP (486.5±16.5). The largest change was noted in the control group (556.2±34.4). For all paired comparisons, statistically significant differences (with $p<0.05$) were observed, with the only exception being a comparison between B+TCP and B+BG+TCP.

5.5 Histopathologic analysis

In all analyzed groups, after 7 days of the study, mandibular bone defects had filled with immature fibrous tissue. Numerous, minute granules of deproteinized human bone (with no signs of activity) were seen in this tissue (group B). Additionally, depending on the implant composition, foggy fractions of bio-glass or linearly cracked deposits of tricalcium phosphate could be seen (in groups B+BG, B+TCP and B+BG+TCP). At the same time, active reconstruction of skeletal tissue was observed at the entire periphery of the bone defects implanted with B, B+TCP and B+BG+TCP, as suggested by the presence of ground substance (osteoid) containing numerous immature bone trabeculae covered with osteoblasts. In controls, as well as in groups B and B+BG, blood clots along with the remnants of necrotic bone trabeculae could be seen in the bone marrow at the base of the bone defect. In groups where bio-glass was implanted into the bone defect (B+BG and B+BG+TCP), fragments of this material formed pseudocystic structures that were covered with a thin connective tissue capsule comprised of fibroblasts, fibrocytes and single giant polynuclear cells.

After two weeks of the experiment, the implanted bone defects were filled with mature fibrous connective tissue that contained collagen fibers. Only in group B could immature connective tissue with numerous blood vessels be seen at the periphery of the defect. Immature bone trabeculae were visible in this tissue, surrounded with osteoblasts. Depending on the implant composition, fragments of deproteinized bone granules, bio-glass and/or tricalcium phosphate were seen in the fibrous connective tissue. Around BG and TCP particles, distinct, thick-walled pseudocystic structures could be observed, containing numerous giant polynuclear cells. Additionally, giant polynuclear cells were frequently visible on the surface of deproteinized bone but they did not form distinct capsule-like linear structures in this location. Fragmentation of some TCP particles could be observed due to infiltration by cells composing the previously mentioned cystic structures. Active osteogenesis was evident in all analyzed groups, as manifested by the pronounced growth of numerous immature bone trabeculae covered with osteoblasts. This process was particularly intensive around the particles of implanted material.

In group B, advanced reconstruction of bone defects was observed after three weeks of the study. Most bone trabeculae filling the defect were mature with either no or very little osteoblastic activity. Linearly placed osteoblasts, or even osteoclasts, could be seen on the surface of remaining trabeculae (Fig. 9). A similar advancement in the bone formation process was observed in B+TCP specimens: osteoid was formed on the base of connective fibrous tissue along with the intensive growth of numerous bone trabeculae. Some of these trabeculae were mature already and showed no signs of cellular activity. Skeletal tissue regeneration in this group was particularly enhanced around the fragments of deproteinized bone and tricalcium phosphate (Fig. 10). In contrast to B particles, TCP particles showed signs of dilution and structural fragmentation. Only a few giant polynuclear cells could be seen around the implants, and the previously observed cystic structures of TCP had only residual character. After three weeks of the study, slightly less advanced processes of skeletal defect healing were observed in histologic specimens from groups B+BG and B+BG+TCP. Growth of immature skeletal tissue was observed in these groups on the "scaffold" of deproteinized bone, giving the impression of the implant being "incorporated" into the growing bone trabeculae. Only single giant polynuclear

cells could be seen on the surface of specimens from group B+BG. Additionally, thin, linearly placed cells could be observed around some bio-glass particles, forming pseudocystic structures. These structures were visible mostly in areas directly adjacent to fibrous connective tissue. Numerous bone trabeculae were observed around the B+BG+TCP mixture particles, as well as in the fibrous connective tissue between the particles (Fig. 11). Some trabeculae were mature and showed no signs of osteoblastic activity on their surfaces. Some implant particles in this group were covered with giant polynuclear cells forming structures resembling foreign body granulomas. In the control group, all osteoid trabeculae were surrounded by osteoblasts still showing signs of osteoblastic activity.

After four weeks of the study, only the bone defects in group B were nearly completely filled with mature, compact skeletal tissue. This tissue contained numerous "incorporated" granules of deproteinized human bone. Growing bone trabeculae with surface signs of osteoblastic activity could only be seen in a narrow layer of fibrous connective tissue located between the newly formed bone and the bottom of the defect. At the same time, mature cancellous skeletal tissue could only be observed at the periphery of bone defects in groups B+TCP and B+BG+TCP. "Incorporated" fragments of the implanted material, mostly human bone, were visible in this tissue. The central part of the defects was still filled with fibrous connective tissue, showing signs of the ongoing process of bone formation. This area also contained B particles and a few particles of TCP ceramic. These fragments of tricalcium phosphate were covered with a pseudo-capsule comprised of giant polynuclear cells, and were gradually fragmented and resorbed. After four weeks of the experiment, numerous mature bone trabeculae with no signs of cellular activity were observed in specimens from group B+BG (Fig. 12). Some of these trabeculae developed around B and BG particles, giving the impression of "incorporating" implanted material into the structure of reconstructed bone. Some bone defects were still partially filled with mature fibrous connective tissue containing numerous collagen fibers along with particles of implanted material. Additionally, pseudocystic structures could be observed around the BG particles, comprised of linearly placed giant polynuclear cells.

Histopathologic examination performed after eight weeks of the study revealed the completed process of bone healing in group B. Bone structure was fully regenerated, and mature compact bone and cancellous bone could be observed at the defect site, along with normal bone marrow (Fig. 13). Observations made in the B+BG+TCP group after the 8th and 12th weeks of the experiment gave similar findings. In this group bone defects were also filled with mature compact and cancellous skeletal tissue, with "incorporated" particles of bio-glass and deproteinized bone still visible (Fig. 14). These particles showed no signs of activity, and were covered with thin fibrous capsules. In the 8th experimental week, these particles could also be observed in fibrous connective tissue. After the 8th week of the study, the process of osteogenesis was still incomplete in B+BG and B+TCP specimens. In defects implanted with bio-glass, some areas, usually peripheral ones, were still filled with fibrous connective tissue containing numerous collagen fibers. This connective tissue showed signs of ongoing bone formation: maturating or mature bone trabeculae, along with bio-glass particles forming pseudocystic structures (Fig. 15). Particles of deproteinized bone were more rarely evidenced. At the same time, continued bone formation was observed in the central part of bone defects in group B+TCP (Fig. 16). This process was particularly

intensive around the B particles, giving the characteristic impression of "incorporating" this material into newly formed bone. After eight weeks of the study, only some bone trabeculae in the control group showed signs of osteoblastic activity, while other areas of the defect contained mature trabeculae.

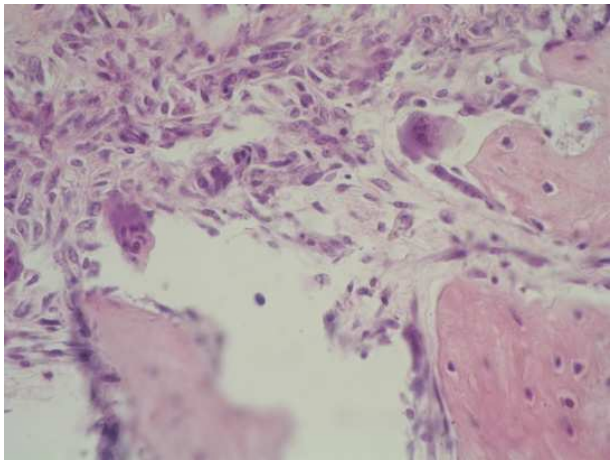

Fig. 9. Histopathologic specimen – 3rd week, group B – single osteoclasts on the surface of bone trabeculae (H&E staining, magnification 400 x)

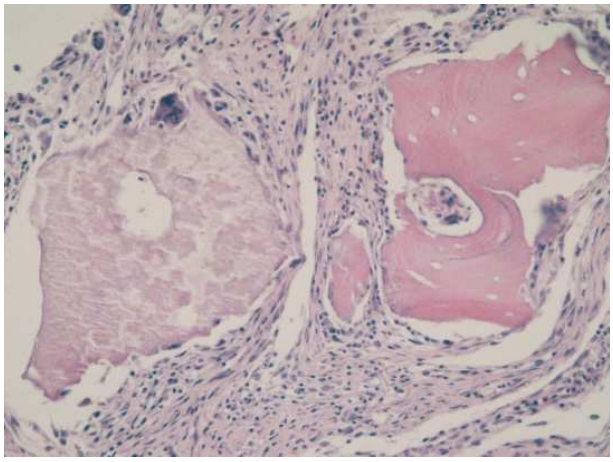

Fig. 10. Histopathologic specimen – 3rd week, group B+TCP – regeneration of skeletal tissue around fragments of deproteinized human bone and tricalcium phosphate (H&E staining, magnification 200 x)

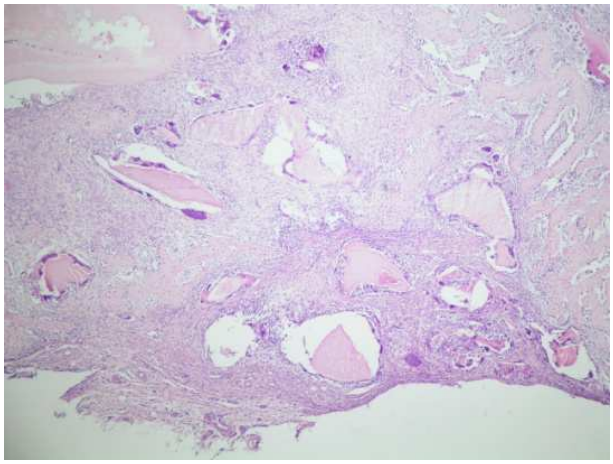

Fig. 11. Histopathologic specimen – 3rd week, group B+BG+TCP – numerous bone trabeculae around the implanted material visible within fibrous connective tissue (H&E staining, magnification 40 x)

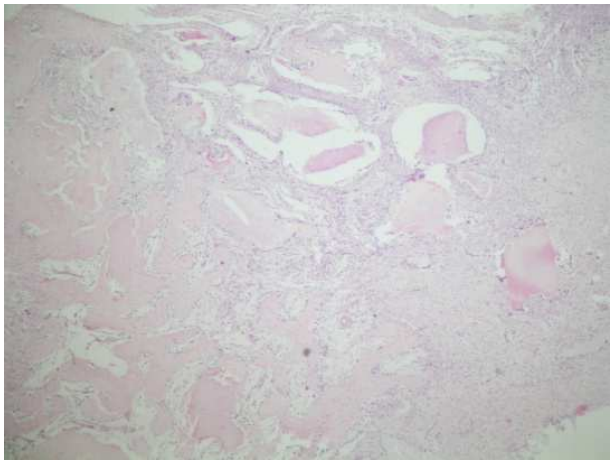

Fig. 12. Histopathologic specimen – 4th week, group B+BG – mature bone trabeculae with no signs of cellular activity, along with particles of deproteinized human bone and bio-glass visible within fibrous connective tissue (H&E staining, magnification 40 x)

After 12 weeks of the study, the process of skeletal tissue regeneration in specimens from groups B+BG and B+TCP was still not complete. Although the defects were nearly filled in their entirety with mature compact and cancellous bone, mature fibrous connective tissue containing numerous collagen fibers and showing signs of ongoing osteogenesis could still be seen in the superficial zone (Fig. 17). This superficial layer contained remnants of deproteinized bone, covered with capsules comprised of giant polynuclear cells, which formed inactive, fibrous foreign body granulomas. Additionally, cystic structures containing foggy remnants of incompletely resorbed TCP (group B+TCP) or BG particles (group B+BG)

were revealed in fibrous connective tissue (Fig. 18). In the control group, specimens obtained in the 12th week of the study contained completely matured and fully mineralized bone.

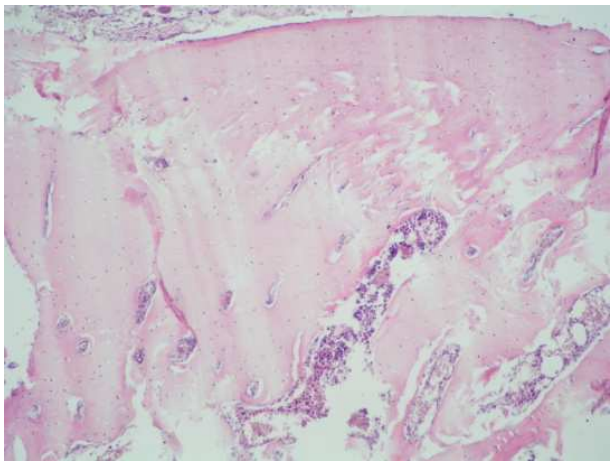

Fig. 13. Histopathologic specimen – 8th week, group B – mature skeletal tissue and bone marrow (H&E staining, magnification 100 x)

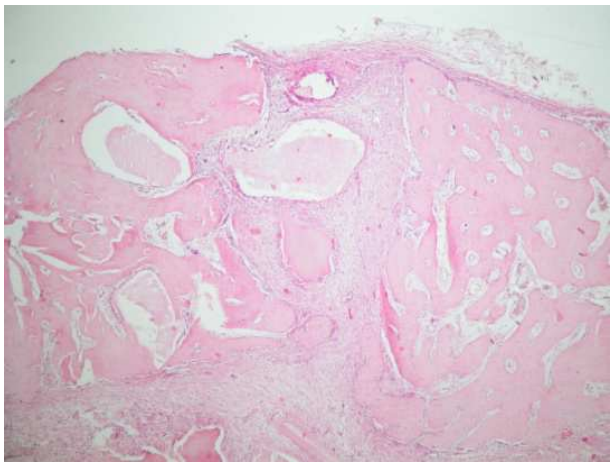

Fig. 14. Histopathologic specimen – 8th week, group B+BG+TCP – mature compact and cancellous skeletal tissue with "incorporated" particles of bio-glass and human bone (H&E staining, magnification 100 x)

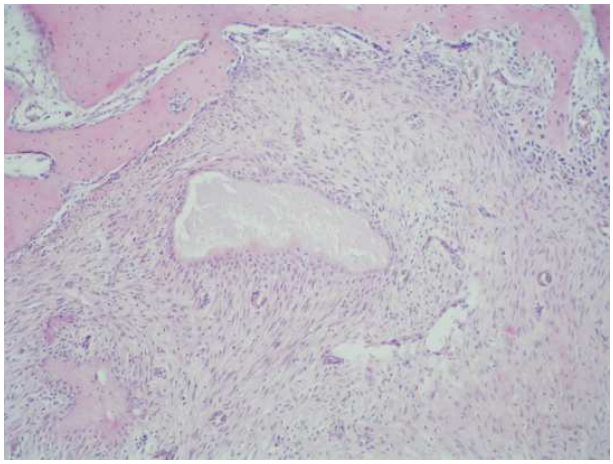

Fig. 15. Histopathologic specimen – 8th week, group B+BG – bio-glass particle forming pseudocystic structure within the mature fibrous connective tissue (H&E staining, magnification 100 x)

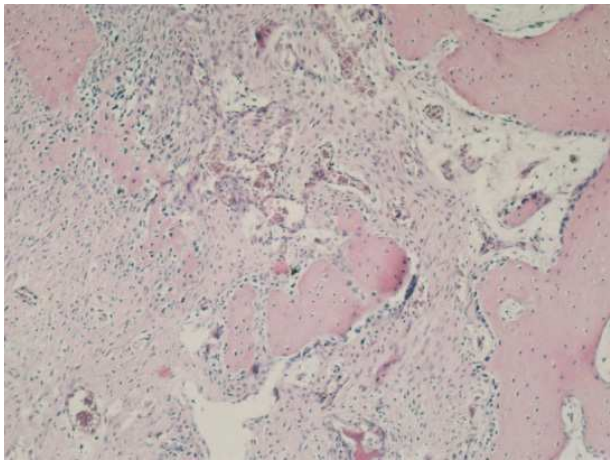

Fig. 16. Histopathologic specimen – 8th week, group B+TCP – fibrous connective tissue with massive osteogenesis (H&E staining, magnification 100 x)

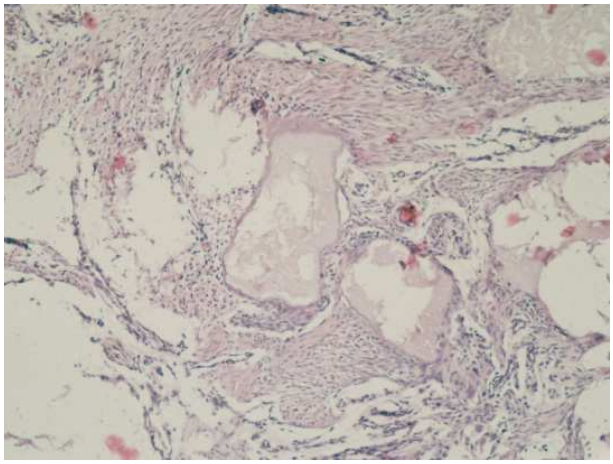

Fig. 17. Histopathologic specimen – 12th week, group B+BG – mature fibrous connective tissue with numerous cystic spaces filled with foggy deposits of bio-glass (H&E staining, 100 x)

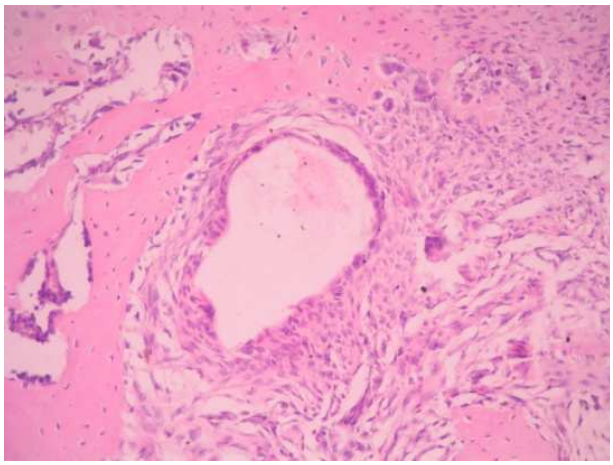

Fig. 18. Histopathologic specimen – 12th week, group B+TCP – cystic structures within fibrous connective tissue containing foggy remnants of tricalcium phosphate (H&E staining, 200 x)

6. Discussion

Due to the limited regenerative ability of skeletal tissue, bone grafting or the implantation of bone derivatives or bone replacement materials is required for the complete healing of large bone defects, whether the result of surgical removal of skeletal cysts or tumors, or caused by other skeletal disorders (Precheur, 2007). The most satisfactory results in stimulating skeletal tissue regeneration have been reported after using autogenous grafts. After being implanted into the bone defect, autogenous grafts can induce all the basic mechanisms responsible for bone reconstruction, i.e. osteogenesis, osteoinduction and osteoconduction (Giannoudis et

al., 2005; Merkx et al., 2003). Osteogenic activity is associated with the presence of osteoprogenitor cells in the periosteum, endosteum and bone marrow. In the case of free bone grafts, some of the cells located most superficially may survive and are involved in regeneration processes. The results of bone healing stimulation are definitely most satisfactory when autogenous cancellous bone chips are implanted, since this type of bone contains a high number of osteoprogenitor cells. Osteogenic activity can only be observed in fresh bone grafts. Osteoinduction is associated with the presence of so-called bone morphogenetic proteins (BMP) in the bone matrix. These proteins are released during bone remodeling, and can stimulate minimally differentiated connective tissue cells surrounding the graft to transform into osteoblasts (Barradas et al., 2011). Both fresh autogenic bone grafts and the allogenic grafts obtained from tissue bank (especially when frozen and partly decalcified) have osteoinductive properties. Additionally, BMP preparations can be obtained by extraction from bones, and as of recent, also by biotechnological synthesis in recombinant form. Allogenic bones are very frequently lyophilized, which depletes them of BMP. Additionally, such grafts lose their immunogenic properties due to irradiation sterilization and deep freezing (Bohner, 2010; Liu et al., 2008). This process of sterilization results in decreased durability of the material, and the preserved bone matrix has only osteoconductive properties. It is degraded by osteoclasts with the simultaneous formation of woven bone, which is further transformed into lamellar bone through the process of osteoclasia. Such grafts have been shown to undergo revascularization and remodeling – similar to autogenous grafts, but at a slower rate. Apart from bone implants, organic and inorganic alloplastic bone replacement materials also have osteoconductive properties. Combined with growth factors and autogenous barrier membranes, they are frequently used as basic elements in the process of guided bone regeneration (GBR) (Kao & Scott, 2007; Schwarz et al., 2007).

For various reasons, different bone materials are frequently combined with each other or with alloplastic biomaterials. As a result, biologically improved material compositions are obtained, some of which positively influence the bone formation processes. Combination of natural hydroxyapatite with chitosane resulted in a composite with osteoconductive properties. In the presence of this composite, tibial consolidation in rabbits was observed as early as 12 weeks after implantation, and complete healing was observed after 16 weeks of the study (Yuan et al., 2008). In another study, a composite based on bovine bone with the addition of bio-glass showed no cytotoxicity to human fibroblasts. Moreover, a crystalline carbonated apatite phase was developed on the sample surface as early as 12 days after immersion in simulated body fluid (Yoganad e al., 2010). Another example of the positive effects of combining deproteinized bovine bone with autogenous bone comes from a study in which such a material was used for the regeneration of bone defects in the frontal part of the porcine skull. The presence of autogenous bone in the mixture was the basis for the osteoinductive properties of the material and the more favorable biological conditions for bone growth when compared to deproteinized bovine bone alone (Thorwarth et al., 2006). Similarly, more satisfactory clinical results were reported when deproteinized bovine bone was used in combination with autogenous bone in the management of alveoschisis in humans, instead of bone autograft alone (Thuaksuban et al., 2010). Experiments on rabbits have also given interesting results. It was revealed that the addition of deproteinized bovine bone to autogenous grafts increased the mean optical density of newly formed skeletal tissue, with a simultaneous decrease in its content in bone defects (skullcap). The opposite

effects were observed when autogenous bone graft was used alone (Pripatnanont et al., 2009). Using a mixture of allogenic bone and deproteinized bovine bone (BioOss®/Orthoblast II®) for the purposes of maxillary sinus lift did not have results as satisfactory as with the application of deproteinized animal bone or synthetic bone (Osteon®) alone. The individual use of one of these two implant materials was associated with a higher percentage of newly formed osseous fraction collected from the lateral sinus at 4 and 6 months post-operatively (Kim et al., 2009).

In this study we have combined allogenic bone with artificially obtained biomaterials (bio-glass – BG, and/or beta-tricalcium phosphate – TCP) in order to form bone replacement material with improved biological characteristics. Reference materials for comparative analysis of the studied mixtures (B+BG, B+TCP, B+BG+TCP) included lyophilized human bone (B) and the clotted blood of experimental animals. Both clinical observations and further macroscopic, radiographic and histopathologic examinations confirmed that bone defects healed normally in the presence of all studied biomaterials. However, the type of implanted mixture modulated the kinetics of bone formation and the quality of newly formed bone. Bone regeneration was induced markedly earlier whenever biologically active bio-glass was included in the implanted mixture (B+BG, B+BG+TCP). In groups where bio-glass was implanted, irregular shadows were observed on radiographic images of the bone defect sites as early as after two weeks of the study. Probably, these radiographic changes resulted from ongoing reparative processes within the bone. This was additionally confirmed on histopathologic analysis, which revealed intense bone formation processes as early as three weeks after the implantation of BG-containing material. However, bone density measurements (BMD and CT bone density) taken in the early period of this study confirmed the superior quality of newly formed bone only in case of the B+BG mixture. It is plausible that the lower bone densities determined for B+BG+TCP implants resulted from the low content of bio-glass in this mixture. Moreover, as confirmed by histopathologic analysis, resorption of beta-tricalcium phosphate contained in B+BG+TCP already began in the early period of this study. Nonetheless, in the later period of this study, increases in BMD and CT bone density of B+BG implanted bone were markedly lower. As a result, after 12 weeks of the experiment, the defects filled with this mixture were characterized by the lowest BMD values, and histopathologic examination confirmed ongoing bone formation. The final result of bone regeneration was markedly better in the case of defects implanted with B+BG+TCP. In the 12th week, histopathologic analysis revealed mature skeletal tissue (both compact and cancellous bone) at the implantation sites, and this finding was confirmed on radiographic examination. Additionally, new bone formed using B+BG+TCP implantation was characterized by the highest BMD and relatively high CT bone density. Therefore, this regenerated bone most closely resembled the normal skeletal tissue of experimental animals of all mixtures examined. In the 12th week of this study, bone formation processes were still observed in B+TCP implanted defects. Although the BMD of tissue formed on the basis of this implant was higher than in the B+BG implanted bone, it was still lower than in the B+BG+TCP group. Notably, in both the 1st and 12th experimental weeks, only slight differences in BMD and CT bone density were observed between the B+TCP and B+BG+TCP mixtures. Undoubtedly, the process of bone defect regeneration was completed the earliest in group B. Histopathologic studies confirmed that bone defects in this group were filled with mature skeletal tissue with no signs of osteoblastic activity as early as after eight weeks of the study. Early completion of skeletal healing was also

confirmed by the radiographic images taken in this group. In the 12th experimental week, BMD of bone defects implanted with human bone alone was higher in comparison to defects filled with B+TCP and B+BG+TCP, in contrast to the early period of this study when BMD and CT bone density in group B were among the highest.

Results of this study suggest that the quality of bone formed in the late period of the experiment was poorest in the control group, as suggested by the low bone density of defects healing on the basis of clotted blood. Since histopathologic studies confirmed that bone formation in controls was complete in week 12, one should not expect further increases in bone density in this group. It is likely that bone density would increase further, however, with prolonged observation of the B+BG and B+TCP groups, since the last densitometric measurements in these groups were taken on incompletely matured bone.

7. Conclusion

This *in vivo* animal study revealed that both lyophilized human bone (B) and mixtures formed on its basis (B+BG, B+TCP, B+BG+TCP) are fully biocompatible materials. We have confirmed that, in the presence of these materials, there is a possibility of forming normal, mature skeletal tissue in mandibular bone defects of guinea pigs. This was possible mostly thanks to the inclusion of deproteinized human bone in analyzed mixtures. Due to its osteoconductive properties, the presence of human bone resulted in favorable biological conditions that promoted skeletal regeneration. Therefore, deproteinized bone formed a scaffold to support the growth of osteogenic cells within the defects. Furthermore, the addition of alloplastic materials, bio-glass and beta-tricalcium phosphate, markedly influenced the rate of bone formation and the quality of newly formed bone. The most satisfactory results were observed in the case of lyophilized human bone mixed with bio-glass and beta-tricalcium phosphate (B+BG+TCP). The group implanted with this material was the only one in which fully matured compact and cancellous bone was observed on histopathologic examination performed after 12 weeks of the study. The particles of bio-glass and beta-tricalcium phosphate included in the mixture induced the processes of bone formation and stimulated the growth of osteogenic cells. As a result of these initiated biological processes, defragmented and resorbed β-TCP was gradually replaced with newly formed skeletal structures. Such a course of bone formation process modulated the quality of newly formed bone, as confirmed by high BMD and CT bone density values determined after 12 weeks in B+BG+TCP implanted defects. As confirmed on histopathologic examination, throughout the three-month period of this study, skeletal regeneration was not completed in defects implanted with B+BG and B+TCP mixtures. This incomplete regeneration was reflected by the lower bone density values observed in these groups when compared to the B+BG+TCP group. In conclusion, the results of this study confirmed our initial assumptions. We have revealed that, in addition to a proper course of bone formation processes, another important outcome in the presence of various bone replacement materials is the high quality of newly formed bone. In our opinion, these two aforementioned results were positively achieved by the mixture of lyophilized human bone with bio-glass and tricalcium phosphate.

8. References

Abu Bakar, M.S., Cheng, M.H.W., Tang, S.M., Yu, S.C., Liao, K., Tan, C.T., Khor, K.A. & Cheang, P. (2003). Tensile Properties, Tension–tension Fatigue and Biological

Response of Polyetheretherketone–hydroxyapatite Composites for Load-bearing Orthopedic Implants. *Biomaterials,* Vol.24, No.13, (July 2003), pp. 2245-2250, ISSN 0142-9612

Accorsi-Mendonça, T., Conz, M.B., Barros, T.C., de Sena, L.Á., de Almeida Soares, G. & Granjeiro, J.M. (2008). Physicochemical Characterization of Two Deproteinized Bovine Xenografts. *Brazilian Oral Research,* Vol.22, No.1, (January-March 2008), pp. 5-10, ISSN 1806-8324

Baldini, N., De Sanctis, M. & Ferrari, M. (2011). Deproteinized Bovine Bone in Periodontal and Implant Surgery. *Dental,* Vol.27, No.1, (January 2011), pp. 61-70, ISSN 1879-0097

Barakat, N.A.M., Khil, M.S., Omran, A.M., Sheikh, F.A. & Kim, H.Y. (2009). Extraction of Pure Natural Hydroxyapatite from the Bovine Bones Bio Waste by Three Different Methods. *Journal of Materials Processing Technology,* Vol.209, No.7, (April 2009), pp. 3408-3415, ISSN 0924-0136

Barradas, A.M.C., Yuan, H., van Blitterswijk, C.A. & Habibovic, P. (2011). Osteoinductive Biomaterials: Current Knowledge of Properties, Experimental Models and Biological Mechanisms. *European Cell and Materials,* Vol.21, (2011), pp. 407-429, ISSN 1473-2262

Bellucci, D., Cannillo, V. & Sola, A. (2011). A New Highly Bioactive Composite for Scaffold Applications: A Feasibility Study. *Materials,* Vol.4, (January 2011), pp. 339-354, ISSN 1996-1944

Block, M.S., Finger, I. & Lytle, R. (2002). Human Mineralized Bone in Extraction Sites Before Implant Placement. *The Journal of the American Dental Association,* Vol.133, No.12, (December 2002), pp. 1631-1638, ISSN 0002-8177

Bohner, M. (2010). Resorbable Biomaterials as Bone Graft Substitutes. *Materials Today,* Vol.13, No.1-2, (January-February 2010), pp. 24-30, ISSN 1369-7021

Cao, K., Huang, W., An, H., Jiang, D., Shu, Y. & Han, Z. (2009). Deproteinized Bone with VEGF Gene Transfer to Facilitate the Repair of Early Avascular Necrosis of Femoral Head of Rabbit. *Chinese Journal of Traumatology (English Edition),* Vol.12, No.5, (October 2009), pp. 269-274, ISSN 1008-1275

Choi, J.W., Cho, H.M., Kwak, E.K., Kwon, T.G., Ryoo, H.M., Jeong, Y.K., Oh, K.S. & Shih, H.I. (2004). Effect of Ag-doped Hydroxyapatite as a Bone Filler for Inflamed Bone Defects. *Key Engineering Materials,* Vol.254-256, (2004), pp. 47-50, ISSN 1013-9826

Cieślik, M., Mertas, A., Morawska-Chochół, A., Sabat, D., Orlicki, R., Owczarek, A., Król, W. & Cieślik, T. (2009). The Evaluation of the Possibilities of Using PLGA co-polymer and Its Composites with Carbon Fibers or Hydroxyapatite in Bone Tissue Regeneration Process – *In Vitro* and *In Vivo* Examinations. *International Journal of Molecular Science,* Vol.10, No.7, (July 2009), pp. 3224-3234, ISSN 1422-0067

Daculsi, G., Laboux, O., Malard, O. & Weiss, P. (2003). Current State of the Art of Biphasic Calcium Phosphate Bioceramics. *Journal of Materials Science Materials in Medicine*, Vol.14, No.3, (March 2003), pp. 195-200, ISSN 0957-4530

Deculsi, G. (1998). Biphasic Calcium Phosphate Concept Applied to Artificial Bone, Implant Coating and Injectable Bone Substitute. *Biomaterials,* Vol.19, No.16, (August 1998), pp. 1473-1478, ISSN 0142-9612

Fellah, B.H., Gauthier, O., Weiss, P., Chappard, D. & Layrolle, P. (2008). Osteogenicity of Biphasic Calcium Phosphate Ceramics and Bone Autograft in a Goat Model. *Biomaterials,* Vol.29, No.9, (March 2008), pp. 1177-1188, ISSN 0142-9612

Ferreira, J.M.F. (2007). Development and In Vitro Characterization of Sol–gel Derived CaO–P_2O_5–SiO_2–ZnO Bioglass. *Acta Biomaterialia,* Vol.3, No.2, (March 2007), pp. 255-262, ISSN 1742-706

Giannoudis, P.V., Dinopoulos, H. & Tsiridis, E. (2005). Bone Substitutes: An Update. Injury, Vol.36, No.3, Supp.1, (November 2005), pp. 20-27,ISSN 0020-1383

Henkel, K.O., Gerber, T., Gundlach, K.K.H. & Bienengräber, V. (2006). Macroscopical, Histological, and Morphometric Studies of Porous Bone-Replacement Materials in Minipigs 8 Months After Implantation. *Oral Surgery, Oral Medicine, Oral Pathology, Oral Radiology, and Endodontology,* Vol.102, No.5, (November 2006), pp. 606-613, ISSN 1079-2104

Jian, Y., Tian, X., Li, B., Qiu, B., Zhou, Z., Yang, Z. & Li, Q. (2008). Properties of Deproteinized Bone for Reparation of Big Segmental Defect in Long Bone. *Chinese Journal of Traumatology (English Edition),* Vol.11, No.3, (June 2008), pp. 152-156, ISSN 1008-1275

Kao, S.T. & Scott, D.D. (2007). A Review of Bone Substitutes. *Oral and Maxillofacial Surgery Clinics of North America,* Vol.19, No.4, (November 2007), pp. 513-521, ISSN 1042-3699

Kim, Y.K., Yun, P.Y., Kim, S.G. & Lim, S.C. (2009). Analysis of the Healing Process in Sinus Bone Grafting Using Various Grafting Materials. *Oral Surgery, Oral Medicine, Oral Pathology, Oral Radiology, and Endodontology,* Vol.107, No.2, (February 2009), pp. 204-211, ISSN 1076-2104

Kon, M., Ishikawa, K., Miyamoto, Y. & Asaoka, K. (1995). Development of Calcium Phosphate Based Functional Gradient Bioceramics. *Biomaterials,* Vol.16, No.9, (June 1995), pp. 709-714, ISSN 2079-4983

Liu, L., Pei, F., Tu, C., Zhou, Z. & Li, Q. (2008). Immunological Study on the Transplantation of an Improved Deproteinized Heterogeneous Bone Scaffold Material in Tissue Engineering. *Chinese Journal of Traumatology (English Edition),* Vol.11, No.3, (June 2008), pp. 141-147, ISSN 1008-1275

Merkx, M.A.V., Maltha, J.C. & Stoelinga, P.J.W. (2003). Assessment of the Value of Anorganic Bone Additives in Sinus Floor Augmentation: A Review of Clinical Reports. *International Journal of Oral and Maxillofacial Surgery,* Vol.32, No.1, (February 2003), pp. 1-6, ISSN 1548-1336

Nagata, F., Miyajima, T. & Yokagawa, Y. (2003). Preparation of Porous Composites Consisting of Apatite and Poly(D,L-lactide). *Key Engineering Materials,* Vol.240-242, (2003), pp. 167-170, ISSN 1013-9826

Nagata, F., Miyajima, T., Teraoka, K. & Yokogawa, Y. (2005). Preparation of Porous Poly(lactic acid)/Hydroxyapatite Microspheres Intended for Injectable Bone Substitutes. *Key Engineering Materials,* Vol.284-286, (2005), pp. 819-822, ISSN 1013-9826

Oonishi, H., Hench, L.L., Wilson, J., Sugihara, F., Tsuji, E., Kushitani, S. & Iwaki, H. (1999). Comparative bone growth behavior in granules of bioceramic materials of various sizes. *Journal of Biomedical Material Research,* Vol.44, No.1, (January 1999), pp. 31-43, ISSN 0021-9304

Precheur, H.V. (2007). Bone Grafts Materials. *Dental Clinics of North America,* Vol.51, No.3, (July 2007), pp. 729-746, ISSN 0011-8532

Pripatnanont, P., Nuntanaranont, T. & Vongvatcharanont, S. (2009). Proportion of Deproteinized Bovine Bone and Autogenous Bone Affects Bone Formation in the Treatment of Calvarial Defects in Rabbits. *International Journal of Oral and Maxillofacial Surgery,* Vol.38, No.4, (April 2009), pp. 356-362, ISSN 1399-0020

Ravarian, R., Moztarzadeh, F., Solati Hashjin, M., Rabiee, S.M., Khoshakhlagh, P. & Tahriri, M. (2010). Synthesis, Characterization and Bioactivity Investigation of Bioglass/Hydroxyapatite Composite. *Ceramics International,* Vol.36, No.1, (January 2010), pp. 291-297, ISSN 0272-8842

Santos, L.A., Carrodeguas, R.G., Rogero, S.O., Higa, O.Z., Boschi, A.O. & Arruda, A.C.F. (2002). α-Tricalcium phosphate cement: "in vitro" cytotoxicity. *Biomaterials,* Vol.23, No.9, (May 2002), pp. 2035-2042, ISSN 2079-4983

Schwarz, F., Herten, M., Ferrari, D., Wieland, M., Schmitz, L., Engelhardt, E. & Becker, J. (2007). Guided Bone Regeneration at Dehiscence-type Defects Using Biphasic Hydroxyapatite + Beta Tricalcium Phosphate (Bone Ceramic®) or a Collagen-coated Natural Bone Mineral (BioOss Collagen®): An Immunohistochemical Study in Dogs. *International Journal of Oral and Maxillofacial Surgery,* Vol.36, No.12, (December 2007), pp. 1198-1206, ISSN 0901-5027

Ślósarczyk, A. & Paszkiewicz, Z. (2005). Method of obtaining highly reactive calcium phosphate powder. Pl Patent 1900486 B1, App. No. 331907, Int. Cl.{7} : C01B 25/32, (December 2005)

Thomas, M.V., Puleo, D.A. & Al-Sabbagh, M. (2005). Bioactive Glass Three Decades on. *Journal of Long-Term Effects of Medical Implants,* Vol.15, No.6, (February 2005), pp. 585-597, ISSN 1050-6934

Thorwarth, M., Schlegel, K.A., Wehrhan, F., Srour, S. & Schultze-Mosgau, S. (2006). Acceleration of de Novo Bone Formation Following Application of Autogenous Bone to Particulated Anorganic Bovine Material *In Vivo*. *Oral Surgery, Oral Medicine, Oral Pathology, Oral Radiology, and Endodontology,* Vol.101, No.3, (March 2006), pp. 309-316, ISSN 1076-2104

Thuaksuban, N., Nuntanaranont, T. & Pripatnanont, P. (2010). A comparison of Autogenous Bone Graft Combined with Deproteinized Bovine Bone and Autogenous Bone Graft Alone for Treatment of Alveolar Cleft. *International Journal of Oral and Maxillofacial Surgery,* Vol.39, No.12, (December 2010), pp. 1175-1180, ISSN 1399-0020

Von Wattenwyl, R., Siepe, M., Arnold, R., Beyersdorf, F. & Schlensak, C. (2011). Sternum Augmentation with Bovine Bone Substitute in the Neonate. *The Annals of Thoracic Surgery,* Vol.91, No.1, (January 2011), pp. 311-313, ISSN 0003-4975

Wang, S., Zhang, Z., Zhao, J., Zhang, X., Sun, X., Xia, L., Chang, Q., Ye, D. & Jiang, X. (2009). Vertical Alveolar Ridge Augmentation with β-tricalcium phosphate and Aautologous Osteoblasts in Canine Mandible. *Biomaterials,* Vol.30, No.13, (May 2009), pp. 2489-2498, ISSN 0142-9612

Wei G. & Ma P.X. (2004). Structure and Properties of Nano-Hydroxyapatite/Polymer Composite Scaffolds for Bone Tissue Engineering. *Biomaterials,* Vol.25, No.19, (August 2004), pp. 4749-4757, ISSN 0142-9612

Xynos, I.D., Hukkanen, M.V., Batten, J.J., Buttery, L.D., Hench, L.L. & Polak. J.M. (2000). Bioglass 45S5 Stimulates Osteoblast Turnover and Enhances Bone Formation *In*

Vitro: Implications and Applications for Bone Tissue Engineering. *Calcified Tissue International,* Vol.67, No.4, (October 2000), pp. 321-329, ISSN 1432-0827

Yoganand, C.P., Selvarajan, V., Cannillo, V., Sola, A., Roumeli, E., Goudouri, O.M., Paraskevopoulos, K.M. & Rouabhia, M. (2010). Characterization and In vitro-bioactivity of Natural Hydroxyapatite Based Bio-glass–ceramics Synthesized by Thermal Plasma Processing. *Ceramics,* Vol.36, No.6, (August 2010), pp.1757-1766, ISSN 0272-8842

Yuan, H., Chen, N., Lü, X. & Zheng, B. (2008). Experimental Study of Natural Hydroxyapatite/Chitosan Composite on Reconstructing Bone Defects. *Journal of Nanjing Medical University,* Vol.22, No.6, (November 2008), pp. 372-375, ISSN 1007-4376

Yuan, H., de Bruijn, J.D., Zhang, X., van Blitterswijk, C.A. & de Groot, K. (2001). Bone Induction by Porous Glass Ceramic Made from Bioglass (45S5). *Journal of Biomedical Materials Research*, Vol.58, No.3, (May 2001), pp. 270-276, ISSN 1549-3296

Zhang, B., Zhao, J. & Liu, M. (2009). Osteoinductive Activity of Demineralized Bone Matrix and Deprotenized Bone Derived from Human Avascular Necrotic Femoral Head. *Chinese Journal of Traumatology (English Edition),* Vol.12, No.6, (December 2009), pp. 379-383, ISSN 1008-1275

Zima, A., Paszkiewicz, Z. & Ślósarczyk, A. (2010). TCP Bioceramics (αTCP, βTCP, BTCP) for Orthopaedic and Stomatological Applications – Preparation and *In Vitro* Evaluation. *Ceramic Materials,* Vol.62, No.1, (2010), pp. 51-55, ISSN 1644-3470

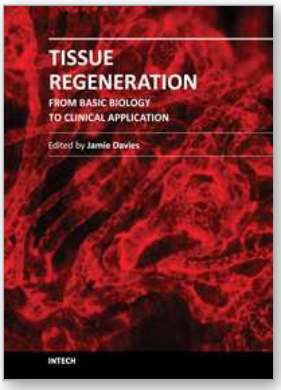

Tissue Regeneration - From Basic Biology to Clinical Application
Edited by Prof. Jamie Davies

ISBN 978-953-51-0387-5
Hard cover, 512 pages
Publisher InTech
Published online 30, March, 2012
Published in print edition March, 2012

When most types of human tissue are damaged, they repair themselves by forming a scar - a mechanically strong 'patch' that restores structural integrity to the tissue without restoring physiological function. Much better, for a patient, would be like-for-like replacement of damaged tissue with something functionally equivalent: there is currently an intense international research effort focused on this goal. This timely book addresses key topics in tissue regeneration in a sequence of linked chapters, each written by world experts; understanding normal healing; sources of, and methods of using, stem cells; construction and use of scaffolds; and modelling and assessment of regeneration. The book is intended for an audience consisting of advanced students, and research and medical professionals.

INTECH
open science | open minds

InTech Europe
University Campus STeP Ri
Slavka Krautzeka 83/A
51000 Rijeka, Croatia
Phone: +385 (51) 770 447
Fax: +385 (51) 686 166
www.intechopen.com

InTech China
Unit 405, Office Block, Hotel Equatorial Shanghai
No.65, Yan An Road (West), Shanghai, 200040, China
中国上海市延安西路65号上海国际贵都大饭店办公楼405单元
Phone: +86-21-62489820
Fax: +86-21-62489821